

Lava fountains during the episodic eruption of South–East Crater (Mt. Etna), 2000: insights into magma-gas dynamics within the shallow volcano plumbing system

D. Andronico · R. A. Corsaro

Received: 8 January 2010 / Accepted: 26 February 2011 / Published online: 16 April 2011
© Springer-Verlag 2011

Abstract Mt. Etna, in Sicily (Italy) is well known for frequent effusive and explosive eruptions from both its summit and flanks. South-East Crater (SE Crater), one of the four summit craters, has been the most active in the last 20 years and often produces episodic lava fountains over periods lasting from a few weeks to months. The most striking of such eruptive phases was in 2000. Sixty four lava fountains, separated by quiescent intervals and sometimes associated with lava overflows, occurred that year between January and June, a time period during which we consider the volcano to have been in episodic eruption. This paper presents mainly results of petrochemical investigations carried out on both tephra and lavas collected during a number of the lava fountain episodes in 2000. The new data have been integrated with volcanological and seismic information in order to correlate the features of the eruptive activity with magma-gas dynamics in the plumbing system of SE Crater. The main findings allow us to characterise the 2000 episodic eruption in the framework of the recent SE Crater activity. In particular, we infer that the onset of the 2000 eruption was triggered by the ascent of new, more primitive and volatile-rich magma that progressively intruded into the SE Crater reservoir, where it mixed with the resident, more evolved magma. Furthermore, we argue that the 2000 SE Crater lava fountains largely resulted from the instability of a foam layer accumulated at the top of the underlying reservoir and rebuilt prior to each episode, in agreement with the collapsing foam model for lava fountains.

Keywords Mt. Etna · Lava fountains · Episodic eruption · Magma mixing · Collapsing foam model

Introduction

Among basaltic volcanoes, Kilauea is certainly known worldwide for its episodic eruptions (Parfitt and Wilson 1994) characterized by sequences of lava fountains (1959–60, 1969–70, 1983–present, see Richter et al. 1970; Swanson et al. 1979; Wolfe et al. 1987, 1988). The episodic behavior of these eruptions has been modeled in terms of non-uniform magma cooling and development of yield strength resulting from variable dike width (Parfitt and Wilson 1994) or physical processes related to the degassing of a magma reservoir (Vergnolle 2008; Vergnolle and Ripepe 2008). Spectacular lava fountain episodes in recent decades have also occurred at Mt. Etna in Sicily, Italy where they may be occasional or, more often, recurrent over periods lasting from a few weeks to months. Lava fountains generally produce eruption columns which cause moderate to abundant tephra fallout up to tens of km from the vent (Alparone et al. 2007). At Mt. Etna, lava fountains commonly take place at the summit of the volcano, where four craters are currently located: North-East Crater, Voragine, Bocca Nuova and South-East Crater (SE Crater) (Fig. 1), though periods of lava fountaining have also been documented from the fissures active during both the 2001 and 2002–03 Mt. Etna flank eruptions.

SE Crater, the youngest summit crater, is the most important expression of high explosivity over the last 20 years at Mt. Etna (Alparone et al. 2003, 2004a, 2007; Behncke et al. 2006). At least five periods of activity have been observed during the growth of the SE Crater: in 1989 (16 lava fountains), in 1998–99 (22), in 2000 (64), and in

Editorial responsibility: R. Cioni

D. Andronico · R. A. Corsaro (✉)
Istituto Nazionale di Geofisica e Vulcanologia,
sezione di Catania, piazza Roma 2,
95123 Catania, Italy
e-mail: corsaro@ct.ingv.it



Fig. 1 A 2004 view from the helicopter of the summit area of Mt. Etna. *NEC* North East Crater; *VOR* Voragine; *BN* Bocca Nuova; *SEC* South East Crater. Photograph by D. Andronico

2001 (15) (Alparone et al. 2004b; Behncke et al. 2006). The last sequence was in 2006, when 18 explosive episodes characterised by strong Strombolian activity to low lava fountaining occurred during the August–December 2006 eruption (Andronico et al. 2009a, b). More recently, in 2007, six paroxysmal events again took place at SE Crater over a relatively wide time span: four between March and May, one in September and the last one in November (Andronico et al. 2008).

This paper focuses on the extraordinary sequence of 64 lava fountain episodes that occurred at SE Crater between 26 January and 24 June 2000 which, according to Alparone et al. (2003) and following the terminology of Parfitt and Wilson (1994), we define as an episodic eruption. It was characterised by recurrent lava fountains with rather variable frequency. For most of the lava fountain episodes, detailed volcanological observations (carried out by means of frequent field surveys and analysis of recordings from the video-camera surveillance network) have been correlated with the pattern of the volcanic tremor (Alparone et al. 2003). This comparison suggested that the 2000 eruption can be separated into two stages (stage 1: from 26 January to 20 February and stage 2: from 23 February to 24 June) characterized by different values for parameters such as the frequency of occurrence, the duration of a lava fountain, and the associated seismic energy release.

The analysis of magmatic gas compositions performed during the 14 June 2000 episode (Allard et al. 2005), combined with melt inclusion data on erupted tephra by Spilliaert et al. (2006), highlighted that the fountains in June 2000 (and probably over the whole eruption) were due to the emptying of a gas foam layer previously accumulated on the top of a magma body emplaced at 1.8 km depth below SE Crater. The occurrence of a shallow reservoir feeding the 2000 SE Crater activity has been confirmed also by Bonaccorso (2006), who studying the tilt change recorded during the 24 June 2000 episode, detected its source in the violent emptying of a small conduit (5–8 m radius) at 1.5–1.9 km depth below the crater. Again, the composition and vesicularity of ejecta emitted during selected lava fountains

allowed Polacci et al. (2006) to propose that these events are driven by the combination of two distinct degassing processes, i.e. foam collapse at the roof of the magma reservoir and syn-eruptive volatile exsolution as magma rises in the conduit. Rheological modeling (Giordano et al. 2010) demonstrates that the occurrence of Strombolian activity and lava fountaining during the 2000 eruption depends on the emission of magma with orders of magnitude differences in effective viscosity.

Previous papers concern various aspects of single lava fountains, but more specific petrologic studies about the magmatic processes governing the entire January–June 2000 eruption are lacking, and also scarce for similar periodic eruptions elsewhere. A previous study at Mt. Etna was made by La Delfa et al. (2001), who analyzed the 22 lava fountains at SE Crater from September 1998 to February 1999. The authors considered each single paroxysm as an eruption and proposed that the 1998–99 ‘periodic eruptions’ were fed by cyclic replenishments and emptying of a shallow storage zone below SE Crater which, in the period between two consecutive episodes, was flushed with a more primitive magma from depth. Privitera et al. (2003) reiterated a similar idea and proposed the existence of a shallow magma batch regularly refilled from depth to explain the one-to-one relationship between the increase of the tremor amplitude and the 16 lava fountains occurring in 1989 at SE Crater.

In this work, we report new petrochemical data for both lavas and tephra collected during the 2000 eruption and compare them with volcanological and seismological data published by Alparone et al. (2003). This background has underpinned new insights into the periodic eruptions of SE Crater in terms of magmatic processes within the plumbing system of Mt. Etna. More generally, the presented results have deepened the knowledge of the most common styles of basaltic explosive activity, i.e. lava fountains, explaining them in term of magma-gas processes occurring in the feeding system of an active volcano.

South–East Crater activity before and during the 2000 eruption

The frequent eruptive activity of SE Crater has caused the gradual formation of an almost 300 m-high cone since 1971, when, during the SE Crater’s birth on the south-eastern summit of Mt. Etna, a degassing-pit formed (Alparone et al. 2004a and references therein). The cone grew rapidly in height between 1989 and 1990, due to frequent, sometimes vigorous, paroxysmal activity. A marked increase of activity occurred after 1996, when almost continuous Strombolian explosions took place at its summit. This period of explosive activity concluded between 15 September 1998 and 4 February 1999, with a sequence of 22 lava fountains.

During the last lava fountain of 4 February, the low eastern slope of the cone was breached, leading to a prolonged, sub-terminal effusive eruption up to 12 November 1999. About 2 months of apparent quiescence preceded the 26 January–24 June 2000 eruption, which consisted of 64 distinct episodes, each one showing the same eruptive pattern subdivided into three main phases (Alparone et al. 2003). The *resumption* phase of explosive activity was characterised by moderate lava effusion at the base of the cone and weak Strombolian bursts at the summit; increases in such eruptive phenomena led to the *paroxysmal* phase, during which the explosive activity evolved to lava fountains (Fig. 2a) forming an eruption plume producing significant tephra fall with vigorous lava output. During the *conclusive* phase all the eruptive phenomena rapidly began to wane and then stopped, with only a very meagre, effusive activity persisting from short fissures on the low slopes of the cone.

The episodes lasted from ~20 min to ~9 h to and were separated by quiescent intervals ranging from 3 h to 10 days. During these intervals, the summit of the cone was characterised only by degassing without any indication of explosive activity. Upon cessation of the 23 February lava fountain, a short fissure opened at the southern foot of SE Crater and remained active until May, producing low lava squeezing and occasional spattering activity (Fig. 2b). Another eruptive fissure (which periodically broke the NE flank of the cone during the lava fountaining) was active for a few days after each lava fountain event in May and June, usually prolonging the output of lava flows at very low rates. As a result, this effusive activity gradually produced two small mounds on the S and NE slopes of SE Crater's cone.

In total, the 2000 eruption produced several lava streams both from the summit and the slopes of the cone and a huge quantity of tephra that (in response to the dominant winds at Mt. Etna) formed a thick wedge south- and eastward of SE Crater, decreasing abruptly in thickness within about 1 km from the foot of the cone. These products almost completely covered all the lava flows emitted from the SE cone during the 22 paroxysmal episodes in 1998–99, while, remarkably, the 2000 lava flows were partially buried by

tephra related to the coeval paroxysmal activity. Alparone et al. (2003) documented an output of $15\text{--}20 \times 10^6 \text{ m}^3$ of lava and $2\text{--}3 \times 10^6 \text{ m}^3$ of tephra.

The frequent lava fountaining caused continuous, often temporary, morphological and structural modifications to the SE Crater's cone; the intense tephra fall from the 64 episodes increased the height of the SE Crater's cone by at least 40 m (Alparone et al. 2003).

Analytical techniques and sampling

During the 2000 eruption, 41 samples were collected from lavas and pyroclasts erupted during both effusive and strong Strombolian/lava fountain activity. We selected 25 of them (hereafter samples 2000 FF) to represent most of lava fountain episodes. After the 26 January sampling, bad weather conditions made sampling unfeasible until 20 February. The characterization of products emitted in 2000 from the SE Crater was completed by analysing two samples erupted after the end of the eruption (hereafter 2000 postFF); one is a bomb ejected on 28 August during a weak lava fountain (sample CSE280800) and the other a lava emitted on 30 November during a quiet effusive activity from the north-east flank of the SE Crater's cone (sample CSE301100).

Modal analyses were performed on selected thin sections by counting 1500 points with a 0.3-mm spacing. The estimated values are in vol. % and are recalculated on a vesicle free basis (Table 1). Mineral compositions were measured at INGV-Catania with a LEO-1430 scanning electron microscope equipped with an Oxford EDS micro-analytical system. Routine analytical conditions are 20 keV acceleration tension, 1.2 nA probe current and XPP data reduction. The accuracy of measurements was checked through replicate analyses of mineral standards (Jarosewich et al. 1980) and the relative errors (1σ) are <1% for SiO_2 , Al_2O_3 and FeO , <0.5% for MgO and CaO and between 2 and 3% for TiO_2 , MnO , Na_2O , K_2O and P_2O_5 (Miraglia 2006). Major (wt%) and trace (ppm) elements of bulk rock (Table 1) have been measured respectively by ICP-OES and ICP-MS at the Centre de Recherches Pétrographiques et

Fig. 2 **a** Spectacular lava fountain episode viewed from Catania (February 2000, photograph by D. Andronico); **b** image recorded on 1 April 2000 by the La Montagnola video-camera, showing continuous degassing and weak effusive activity from the fissure that opened in February 2000 at the foot of SE Crater

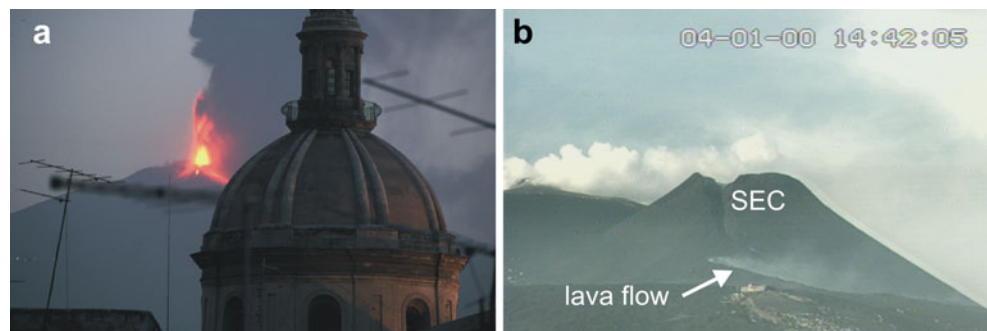


Table 1 Modal composition, chemistry of major and trace elements for the products of the 2000 SE Crater activity

sample	CSE260100A	CSE260100B	CSE200200	CSE280200	CSE040300	CSE080300	CSE120300	CSE140300	CSE290300	CSE010400	CSE160400A	CSE160400B	CSE260400	CSE150500A	CSE150500B	CSE180500
eruption date	26 Jan	26 Jan	20 Feb	28 Feb	4 Mar	8 Mar	12 Mar	14 Mar	29 Mar	1 Apr	16 Apr	16 Apr	26 Apr	15 May	15 May	17 May
type	lava flow	pyroclast	lava flow	lava flow	lava flow	lava flow	lava flow	lava flow	lava flow	lava flow	lava flow	pyroclast	reomorphic lava	lava flow	pyroclast	lava flow
SiO ₂	48.12	47.84	47.25	46.86	46.89	46.84	47.16	46.77	47.01	47.26	46.90	47.08	47.00	46.68	47.16	46.74
TiO ₂	1.59	1.59	1.73	1.70	1.71	1.71	1.70	1.71	1.69	1.71	1.70	1.71	1.70	1.70	1.71	1.71
Al ₂ O ₃	17.92	17.89	17.23	17.08	17.20	17.14	17.19	17.19	17.17	17.23	17.06	17.06	17.01	16.97	17.21	16.91
Fe ₂ O ₃	1.66	1.66	1.77	1.76	1.76	1.75	1.75	1.75	1.74	1.75	1.75	1.75	1.76	1.78	1.76	1.76
FeO	8.30	8.31	8.85	8.80	8.80	8.72	8.75	8.77	8.71	8.76	8.77	8.74	8.78	8.88	8.81	8.78
MnO	0.17	0.18	0.18	0.17	0.17	0.18	0.18	0.18	0.17	0.18	0.18	0.18	0.17	0.17	0.18	0.18
MgO	4.94	5.03	5.81	5.96	5.80	5.72	5.69	5.71	5.70	5.87	5.75	5.84	5.93	6.01	5.71	6.09
CaO	10.12	9.95	10.95	11.02	11.05	10.86	10.89	10.79	10.86	10.91	10.97	11.06	11.03	11.07	11.13	11.13
Na ₂ O	3.86	3.84	3.53	3.51	3.54	3.58	3.56	3.52	3.55	3.62	3.51	3.52	3.45	3.44	3.56	3.39
K ₂ O	2.19	2.14	2.02	2.06	2.05	2.00	2.05	2.02	2.08	2.08	2.11	2.08	2.07	2.05	2.04	1.98
P ₂ O ₅	0.56	0.53	0.54	0.51	0.51	0.51	0.52	0.51	0.52	0.51	0.53	0.49	0.50	0.48	0.50	0.49
L.O.I.	0.57	0.57	0.60	0.56	0.50	0.79	0.52	0.78	0.79	0.52	0.76	0.59	0.60	0.75	0.70	0.50
TOT	100.01	99.53	100.45	99.99	99.98	99.80	99.98	99.81	99.97	100.40	99.99	100.10	99.99	99.97	100.24	99.66
CaO/Al ₂ O ₃	0.56	0.56	0.64	0.65	0.64	0.63	0.63	0.63	0.63	0.63	0.64	0.65	0.65	0.65	0.63	0.66
^a Mg#	0.47	0.48	0.50	0.51	0.50	0.50	0.50	0.50	0.50	0.50	0.50	0.50	0.51	0.51	0.49	0.51
plagioclase	26.5		9.4			13.0			8.5				3.7			8.6
clinopyroxene	9.8		9.6			10.2			8.6				6.5			7.3
olivine	1.6		1.8			3.1			3.0				2.6			1.1
Ti-magnetite	3.2		0.2			0.3			0.1				0.0			0.5
^c P.I.	41.1		21.1			26.7			20.1				12.8			17.5
^d pl/mafic	1.8		0.8			0.9			0.7				0.4			1.0
Rb	48.2	48.8	45.5	45.2	43.9	44.7	45.9	44.2	44.8	46.0	47.6	49.8	47.2	46.5	46.3	45.7
Cs	0.9	0.9	0.8	0.8	0.8	0.8	0.8	0.8	0.8	0.8	0.8	1.1	0.9	0.8	0.8	0.8
Sr	1133	1153	1079	1067	1056	1085	1097	1065	1081	1102	1124	1129	1099	1089	1110	1099
Ba	624	628	570	564	555	564	577	559	566	577	593	576	575	562	582	565
Ta	2.6	2.5	2.3	2.3	2.3	2.3	2.4	2.3	2.3	2.4	2.4	2.3	2.3	2.3	2.4	2.3
Th	8.1	8.0	6.7	6.7	6.6	6.8	6.9	6.8	6.7	7.0	6.9	6.7	6.7	6.5	7.0	6.5
U	2.4	2.4	2.0	2.0	2.0	2.0	2.0	2.0	2.0	2.1	2.0	2.0	2.0	1.9	2.1	1.9
Zr	194	195	179	178	175	179	193	185	189	195	196	195	192	189	193	191
Hf	4.4	4.4	4.2	4.1	4.1	4.1	4.2	4.0	4.1	4.2	4.2	4.2	4.2	4.2	4.2	4.3
Nb	41.5	42.2	37.1	36.1	36.0	36.2	37.0	35.9	36.0	37.1	37.7	36.8	36.4	35.6	37.2	35.7
La	57.2	57.0	51.0	50.6	50.0	50.5	51.9	50.1	50.8	52.1	53.1	51.5	51.0	49.8	52.3	50.2
Ce	110	111	100	99	98	99	101	98	100	102	103	102	100	98	102	99
Nd	46.5	46.9	44.4	44.1	43.3	43.8	44.6	42.9	43.5	44.9	45.6	45.1	44.6	44.1	45.3	44.5
Sm	8.8	8.8	8.7	8.6	8.4	8.5	8.7	8.4	8.4	8.7	8.9	8.8	8.7	8.7	8.8	8.8
Eu	2.7	2.7	2.7	2.7	2.6	2.6	2.7	2.5	2.6	2.7	2.7	2.7	2.7	2.6	2.7	2.7
Tb	0.97	0.98	0.98	0.97	0.95	0.96	0.97	0.94	0.95	0.99	1.00	1.01	0.99	0.97	0.99	1.00
Yb	2.11	2.14	2.11	2.10	2.03	2.05	2.05	2.02	2.06	2.10	2.14	2.11	2.07	2.12	2.12	2.12
Lu	0.3	0.3	0.3	0.3	0.3	0.3	0.3	0.3	0.3	0.3	0.3	0.3	0.3	0.3	0.3	0.3
Y	25.2	25.7	25.2	24.7	24.7	25.2	25.6	24.6	25.0	25.8	26.3	26.4	25.9	25.6	25.8	26.0
Ni	21	21	29	29	29	28	28	28	29	30	31	33	32	33	29	34
Cr	22	23	37	40	40	36	34	35	40	37	38	42	40	45	34	43
V	262	267	299	296	290	301	299	291	300	303	314	317	308	313	305	313
Co	33.4	34.3	38.7	38.7	37.2	38.9	38.5	38.0	38.2	39.0	39.9	41.2	39.5	40.0	38.8	40.5
Cu	117	119	143	142	137	143	142	137	140	146	146	216	144	146	144	138

^a Mg# Mg/(Mg+Fe²⁺) moles, assuming Fe³⁺/Fe²⁺=0.2; ^b plagioclase content (%vol) of phenocrysts recalculated on a vesicle-free basis; ^c P.I. Porphyrinity Index;

^d pl/mafic plagioclase/(clinopyroxene+olivine+Ti-magnetite)

Table 1 (continued)

sample eruption type	CSE200500 20 May lava flow	CSE230500 23 May lava flow	CSE270500 27 May pyroclast	CSE010600A 1 Jun lava flow	CSE010600B 1 Jun pyroclast	CSE080600A 8 Jun lava flow	CSE080600B 8 Jun pyroclast	CSE140600 14 Jun lava flow	CSE240600 24 Jun lava flow	CSE280800 28 Aug pyroclast	CSE301100 30 Nov pyroclast
SiO ₂	47.02	47.09	46.69	47.01	47.29	46.93	46.90	47.01	46.87	47.89	47.28
TiO ₂	1.70	1.72	1.69	1.69	1.70	1.71	1.70	1.70	1.69	1.67	1.65
Al ₂ O ₃	17.10	17.18	16.98	17.18	17.24	17.03	17.20	17.14	17.18	17.61	17.66
Fe ₂ O ₃	1.75	1.77	1.76	1.75	1.75	1.75	1.75	1.75	1.74	1.71	1.71
FeO	8.74	8.83	8.82	8.75	8.75	8.74	8.75	8.74	8.71	8.54	8.53
MnO	0.17	0.17	0.17	0.17	0.18	0.18	0.18	0.18	0.17	0.18	0.18
MgO	5.84	5.78	6.02	5.70	5.80	5.72	5.78	5.77	5.78	5.27	5.28
CaO	11.00	10.90	10.99	10.87	10.93	10.89	10.98	10.96	10.90	10.44	10.41
N ₂ O	3.53	3.55	3.48	3.62	3.56	3.55	3.55	3.58	3.60	3.79	3.82
K ₂ O	2.06	2.04	2.05	2.08	2.03	2.07	2.03	2.09	2.05	2.13	2.15
P ₂ O ₅	0.50	0.48	0.50	0.52	0.49	0.51	0.52	0.50	0.48	0.53	0.57
L.O.I.	0.56	0.48	0.83	0.64	0.49	0.59	0.73	0.58	0.81	0.62	0.75
TOT	99.97	99.99	99.98	99.98	100.22	99.64	100.12	100.00	99.98	100.38	99.99
CaO/Al ₂ O ₃	0.64	0.63	0.65	0.63	0.63	0.64	0.64	0.64	0.63	0.59	0.59
^a Mg#	0.50	0.50	0.51	0.50	0.50	0.50	0.50	0.50	0.50	0.48	0.48
^b plagioclase		11.4		8.5		9.6		8.7	7.6		15.7
clinopyroxene		9.4		7.3		8.7		5.9	7.3		9.7
olivine		3.7		1.1		1.6		3.1	2.4		2.1
Ti-magnetite		0.5		0.0		0.2		0.3	0.3		0.4
^c Pl		24.9		16.9		20.1		18.0	17.6		28.0
^d pl/mafic		0.8		1.0		0.9		0.9	0.8		1.3
Rb	46.3	47.4	45.6	47.1	46.1	46.2	46.0	46.8	47.2	48.8	47.4
Cs	0.8	0.8	0.8	0.8	0.8	0.8	0.8	0.8	0.8	0.9	0.9
Sr	1110	1119	1090	1118	1113	1094	1095	1105	1121	1154	1149
Ba	584	583	567	588	586	570	570	586	586	629	621
Ta	2.3	2.4	2.4	2.4	2.4	2.4	2.4	2.4	2.4	2.5	2.5
Th	6.9	7.0	6.7	7.1	7.0	7.0	7.0	7.0	6.9	8.0	7.7
U	2.0	2.0	2.0	2.1	2.0	2.1	2.1	2.1	2.1	2.4	2.3
Zr	192	196	190	196	195	192	191	194	195	204	204
Hf	4.3	4.3	4.3	4.3	4.3	4.3	4.3	4.4	4.3	4.4	4.4
Nb	37.0	37.5	36.3	37.5	37.3	36.6	36.3	37.6	37.1	39.7	43.0
La	51.9	52.6	51.0	54.1	52.3	53.3	53.0	53.7	53.3	56.7	56.7
Ce	101	102	100	102	101	100	100	102	102	109	108
Nd	45.2	45.8	44.4	45.3	45.3	44.6	44.7	45.2	45.0	47.0	46.7
Sm	8.8	9.0	8.8	8.8	8.8	8.7	8.8	8.9	8.9	9.0	9.0
Eu	2.7	2.7	2.7	2.7	2.7	2.7	2.7	2.7	2.7	2.7	2.7
Tb	1.00	1.02	0.99	1.03	1.01	1.04	1.05	1.06	1.06	0.98	1.01
Yb	2.11	2.15	2.07	2.15	2.09	2.12	2.13	2.15	2.16	2.14	2.13
Lu	0.3	0.3	0.3	0.3	0.3	0.3	0.3	0.3	0.3	0.3	0.3
Y	25.8	26.4	25.7	26.0	26.0	25.7	25.7	26.1	25.9	26.4	26.4
Ni	30	31	31	29	30	30	30	30	31	24	28
Cr	45	50	38	36	39	40	37	39	44	26	31
V	301	312	300	299	298	301	298	308	305	285	285
Co	38.1	39.4	38.7	39.1	38.3	39.0	38.5	39.6	40.0	36.6	38.1
Cu	142	142	143	145	145	144	144	144	143	131	133

Géochimiques (CRPG-CNRS), Nancy, France. Analytical uncertainty (1σ) is: <1% for SiO_2 and Al_2O_3 , <2% for Fe_2O_3 , MgO , CaO , Na_2O , K_2O , <5% for MnO and TiO_2 and 5–10% for P_2O_5 , and <5% for all trace elements except U (<8%).

Petrography and mineral chemistry

The 2000 FF tephra and lavas, except the ones erupted during the 26 January fountain, are moderately porphyritic (Porphyricity Index, P.I., from 13 to 27 vol.%), with prevalent mafic minerals (pl/mafic= plagioclase/(clinopyroxene+olivine+oxide) is between 0.4 and 1.0) and are similar to the products emitted on 4 February 1999, at the beginning of the SE Crater sub-terminal eruption (P.I.=19 vol.% and pl/mafic=0.7, Corsaro, 2010 unpublished work). Most of 2000 FF products, then, differ significantly from the crystal-rich and plagioclase dominant volcanics erupted from the SE Crater between 1997 and 1998 (average P.I.= 31 ± 8 vol.% and pl/mafic= 1.7 ± 0.5 , Corsaro and Pompilio 2004; Corsaro, 2010 unpublished work).

The products of the first lava fountain (on 26 January) are different from the other 2000 FF ones, in being more porphyritic (P.I.=41 vol.%) and with prevailing plagioclase (pl/mafic=1.8), sharing the modal mineralogy of the 1997–98 samples. The pyroclasts (sample CSE301100) emitted in November show P.I.=28 vol.% and pl/mafic=1.3 (Table 1) which make them akin to the products erupted from the SE Crater before (1997–98) and at the onset (on 26 January) of the 2000 eruption.

Mineral chemistry has been performed to analyze the variation of plagioclase and olivine compositions through time, by selecting four samples (26 January, 4 March, 16 April and 15 May) covering most of the eruption. Measurements have been performed on cores and rims of phenocrysts ranging 500–1500 μm in size and on groundmass microlites.

Phenocrysts of the 26 January lava fountain are commonly euhedral, show sieve textures, and generally exhibit normal zoning. About 60% of plagioclase phenocrysts have core composition ranging from An_{63} to An_{78} and 50% of the rims have compositions in the interval An_{48-53} (Fig. 3a). Almost all the microlites range An_{53-63} (Fig. 3a). Olivine crystals are unzoned. Core compositions are Fo_{64-68} and rims are comparable with the composition of groundmass microlites (about 80% microlites are Fo_{66-68} , Fig. 3b). The composition of phenocrysts and groundmass microlites in 4 March and 16 April samples exhibits a wider compositional range and a shift toward more mafic compositions (Fig. 3c and d) than those of the 26 January sample. In fact, the phenocrysts' cores are significantly more An-rich (about 70% crystals with An_{68-83} , Fig. 3c) and forsteritic about 65% is Fo_{68-72} , and the remaining 35% have compositions with $\text{Fo}>74$ that are not present in 26 January sample

(Fig. 3d). Also the most frequent An content measured in the rims (58–63, Fig. 3c) and the Fo content in microlites (68–70, Fig. 3d) proved more primitive than their counterparts in the 26 January sample. Furthermore, in March–April samples, a few phenocrysts with euhedral edges show oscillatory and reverse zoning respectively in plagioclase (Fig. 4a) and olivine (Fig. 4b). The tendency to crystallize progressively more mafic minerals over time is most strongly exhibited in the sample collected on 15 May, in which about 80% of phenocryst cores have compositions An_{78-88} (Fig. 3e) and 45% show a Fo contents >76 (Fig. 3f). The most frequent Fo composition (Fig. 3f) both in the rims (50% crystals with Fo_{74-80}) and in the microlites (50% crystals with Fo_{70-72}) is higher than its counterpart in March–April products. In 15 May samples, numerous phenocrysts of plagioclase with resorbed cores show complex oscillatory zoning (Fig. 4c); reverse zoning in anhedral olivine crystals also occurs (Fig. 4d).

Bulk rock compositions

Following the Total Alkali-Silica (TAS) diagram (Le Maitre 2002), the 2000 FF products are classified as potassic trachybasalts. Variation diagrams plotting parameters indicative of magma evolution ($\text{Mg}\# = \text{Mg}/(\text{Mg} + \text{Fe}^{2+})$ moles, assuming $\text{Fe}^{3+}/\text{Fe}^{2+} = 0.2$ and Th) vs. selected major (Fig. 5a and b) and trace elements (Fig. 5c and d), provide evidence that almost all the 2000 FF volcanics belong to a fairly homogeneous cluster, with the exception of the 26 January samples (Fig. 5) which represent the most evolved products of the 2000 eruption (average of samples CSE260100A and CSE260100B: $\text{Mg}\# = 0.47$; $\text{CaO} = 10.03\%$; alkali=6.01%; $\text{Rb} = 48.5$; $\text{Ni} = 21$; $\text{Th} = 8.0$). The volcanic products erupted from February up to June 2000 are clearly distinct from the 26 January ones, since they are evidently more primitive (average of 23 samples: $\text{Mg}\# = 0.50\pm 0.01$; $\text{CaO} = 10.95\pm 0.08\%$; alkali= $5.59\pm 0.07\%$; $\text{Rb} = 46.2\pm 1.3$; $\text{Ni} = 30\pm 2$; $\text{Th} = 6.8\pm 0.2$). The products emitted from SE Crater after the end of the 2000 eruption, namely 2000 postFF, are similar to those erupted on 26 January and show more evolved compositions (average of samples CSE280800 and CSE301100: $\text{Mg}\# = 0.48$; $\text{CaO} = 10.42\%$; alkali=5.95%; $\text{Rb} = 48.1$; $\text{Ni} = 26$; $\text{Th} = 7.8$) than the other 2000 FF products.

If compared with literature data concerning previous SE Crater activity, the products erupted between February and June 2000 are slightly more primitive (Fig. 5) than those emitted on 4 February 1999, at the beginning of the SE Crater's sub-terminal eruption (La Delfa et al. 2001; Corsaro and Pompilio 2004, Corsaro, 2010 unpublished work). On the other hand, the 26 January and the 2000 postFF products overlap (Fig. 5a and b) the compositional cluster represent-

ing the 1997–98 SE Crater eruptions in the literature (La Delfa et al. 2001; Corsaro and Pompilio 2004).

The temporal variations of major (Figs. 6a and 7a) and trace (Fig. 6b and c) elements and of incompatible trace element ratios (Fig. 6d and e) show that the most evolved (average values: Mg#=0.47, Ni=21, Th=8.0, K/Th*10³=2.24, Rb/Nb=1.16) and most primitive magma (average values: Mg#=0.51, Ni=32, Th=6.7, K/Th*10³=2.52, Rb/Nb=1.28) of the 2000 SE Crater eruption were erupted respectively on 26 January and 15–17 May. In detail, in the period 26 January–17 May, we observe an overall and rather gradual increase of compatible components (i.e. Mg#, CaO/Al₂O₃ and Ni; Figs. 6a and b and 7a) and of ratios between trace elements that are unaffected by fractional crystallization (K/Th*10³; Fig. 6d and e). Conversely, in the same

period the values of the incompatible elements (i.e. Th; Fig. 6c) decrease. Finally, it is noteworthy that after 15–17 May and up to the end of the eruption, the products shift toward more evolved compositions (Figs. 5 and 6).

Discussion

Relationships among volcanological, seismic and compositional data of the 2000 South–East Crater eruption

As noted in the Introduction, a number of volcanological and seismic parameters indicate that the 2000 episodic eruption was characterised by two main stages (Alparone

Fig. 3 Compositions of plagioclase and olivine expressed respectively as An (mol%) and Fo (mol%), measured in phenocrysts (core and rim) and groundmass microlites of samples erupted on 26 January (a, b) 4 March–16 April (c, d) and 15 May (e, f)

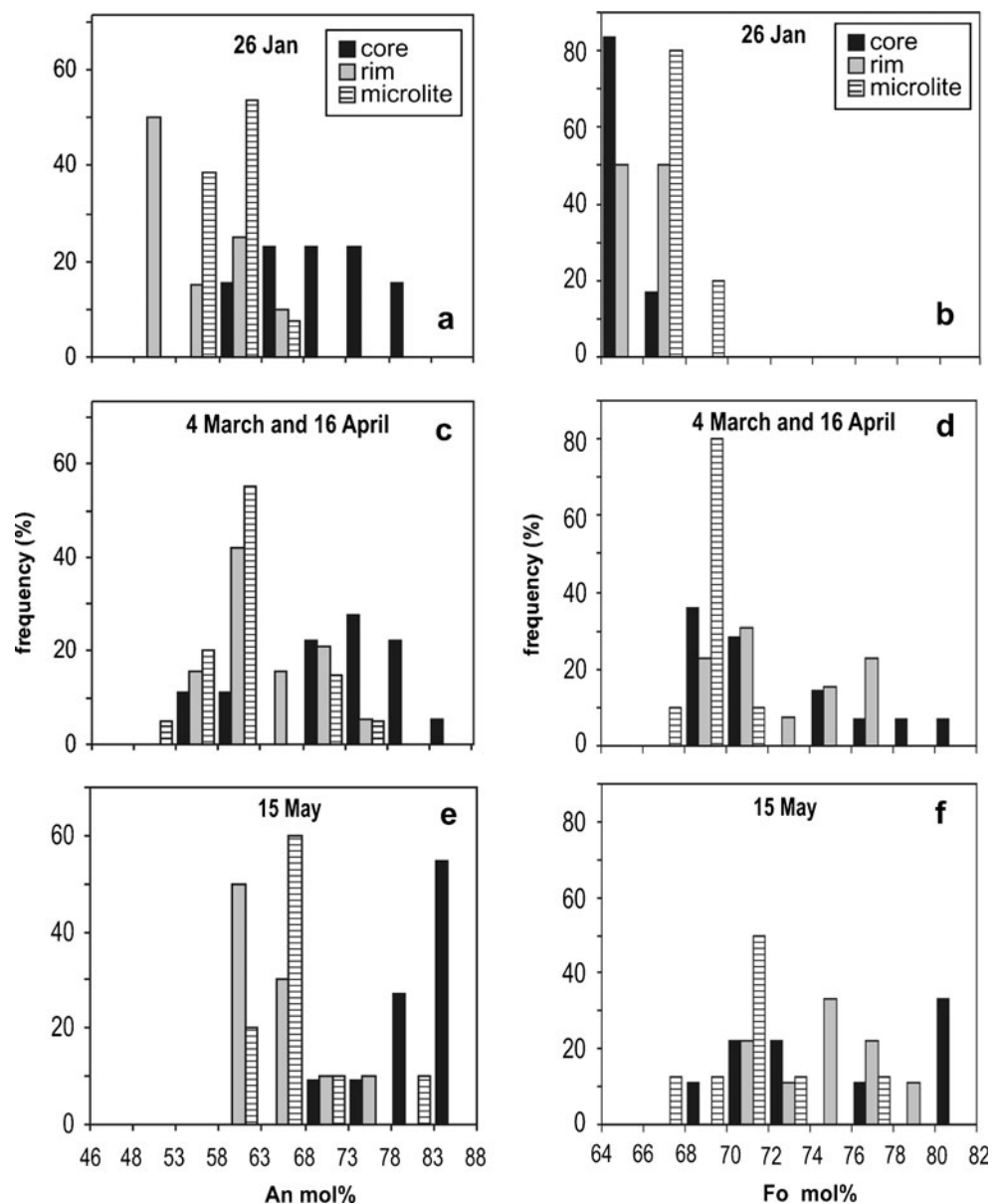


Fig. 4 Petrography of 2000 SE Crater eruption products. SEM back scattered images of: **a** euhedral plagioclase phenocryst with oscillatory zoning, sample CSE040300; **b** euhedral olivine with reverse zoning, sample CSE160400; **c** anhedral plagioclase with abundant sieve textures in the core, showing oscillatory zoning, sample CSE150500; **d** anhedral olivine with reverse zoning, sample CSE150500

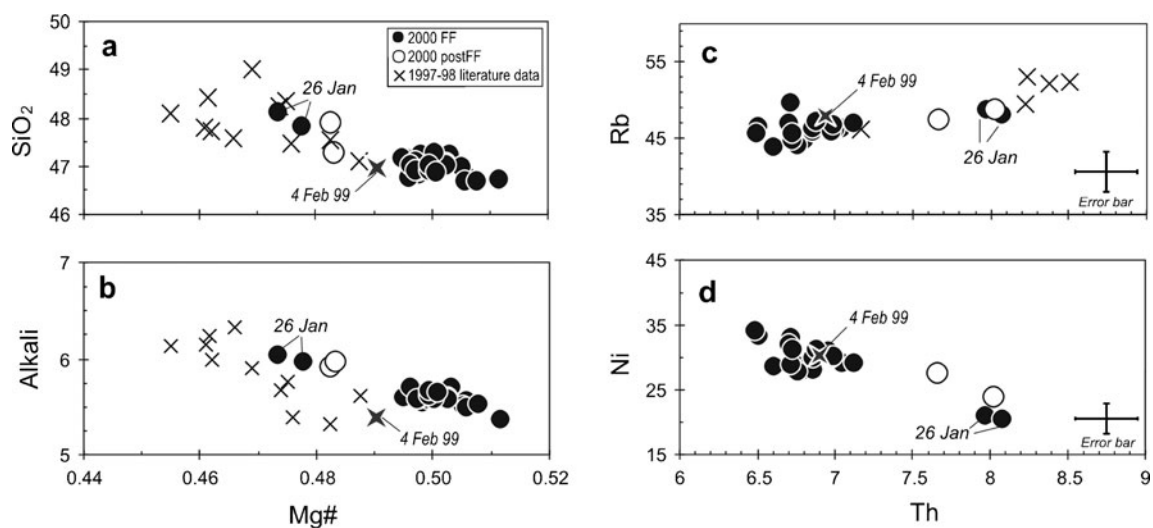
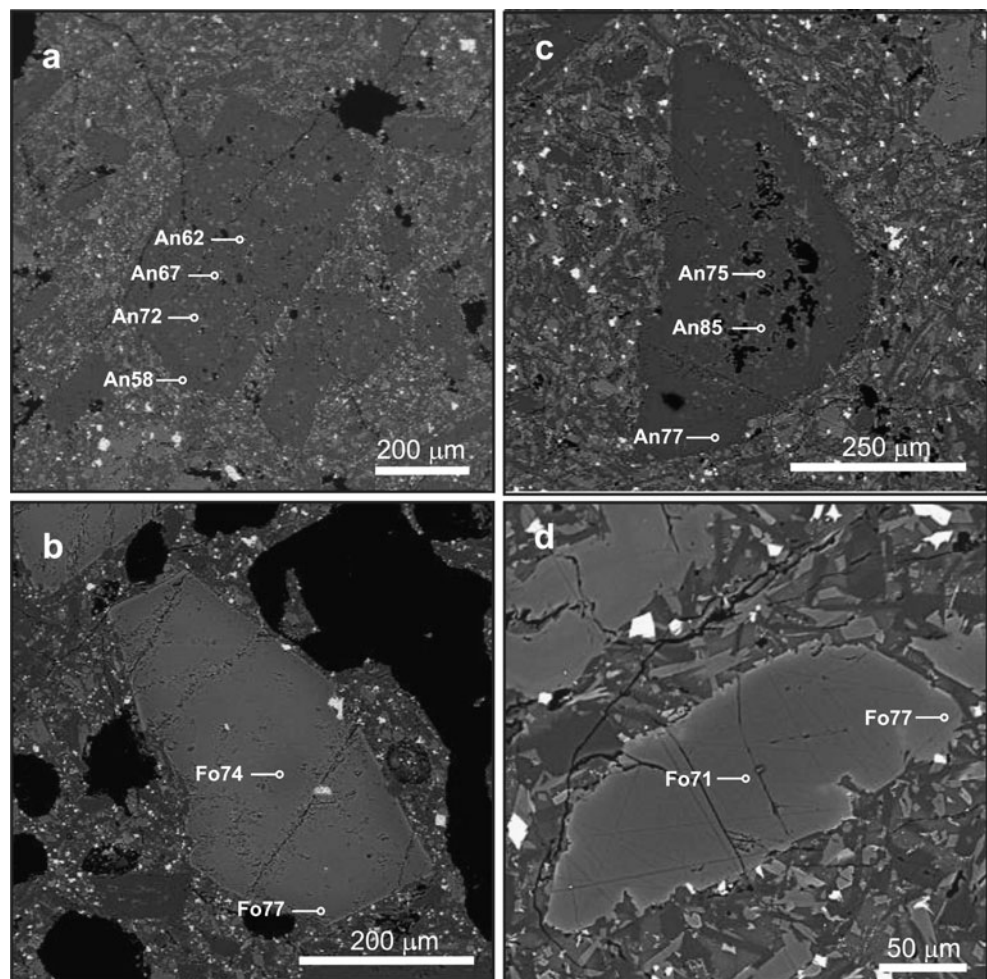


Fig. 5 Variation diagrams of selected majors (**a**, **b**) and trace elements (**c**, **d**) in bulk rocks of products erupted during (2000 FF) and after (2000 postFF) the 2000 SE Crater eruption. $Mg\# = Mg/(Mg + Fe^{2+})$

moles, assuming $Fe^{3+}/Fe^{2+} = 0.2$. Literature data are from La Delfa et al. (2001), Corsaro and Pompilio (2004) and Corsaro (2010, unpublished work) and concern the SE Crater activity from 1997 to 1998

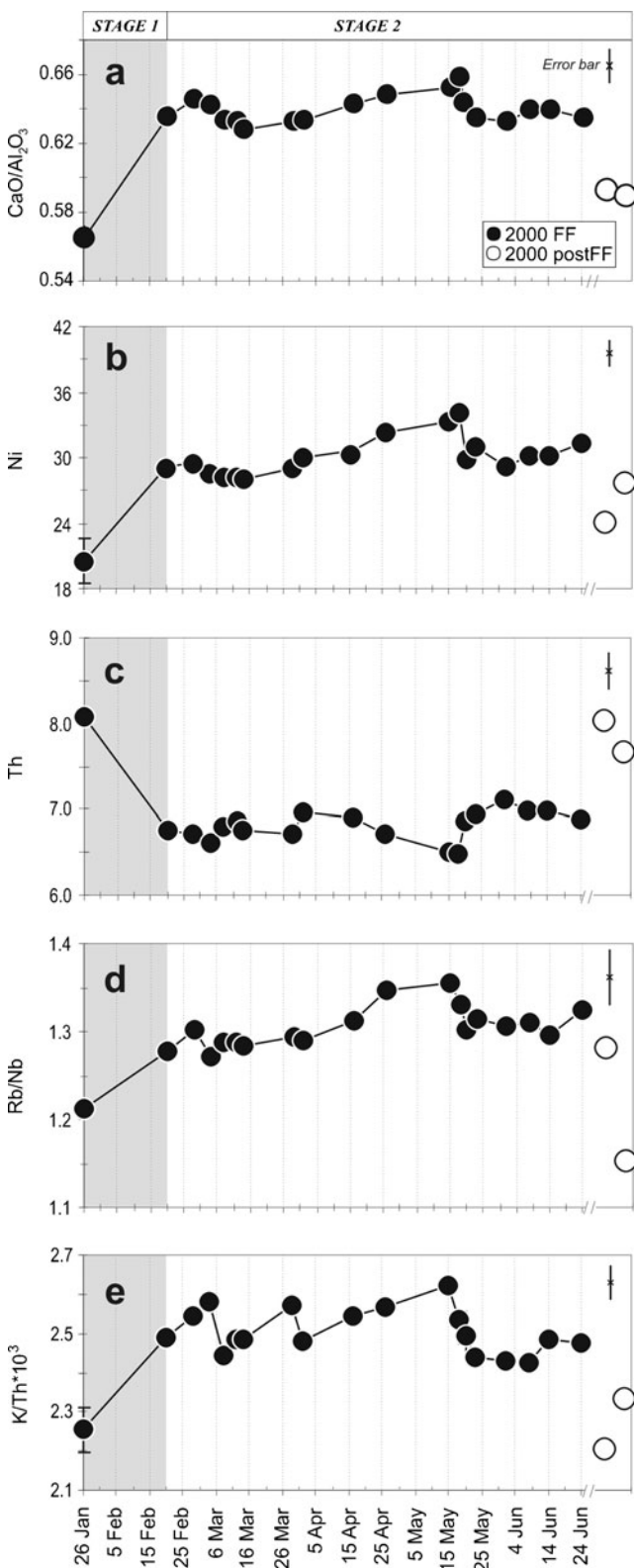


Fig. 6 Temporal variations of selected major (a) and trace (b, c) elements, and ratio between trace elements (d, e) in 2000 FF lavas and 2000 postFF products. Stages 1 and 2 are defined according to Alparone et al. (2003)

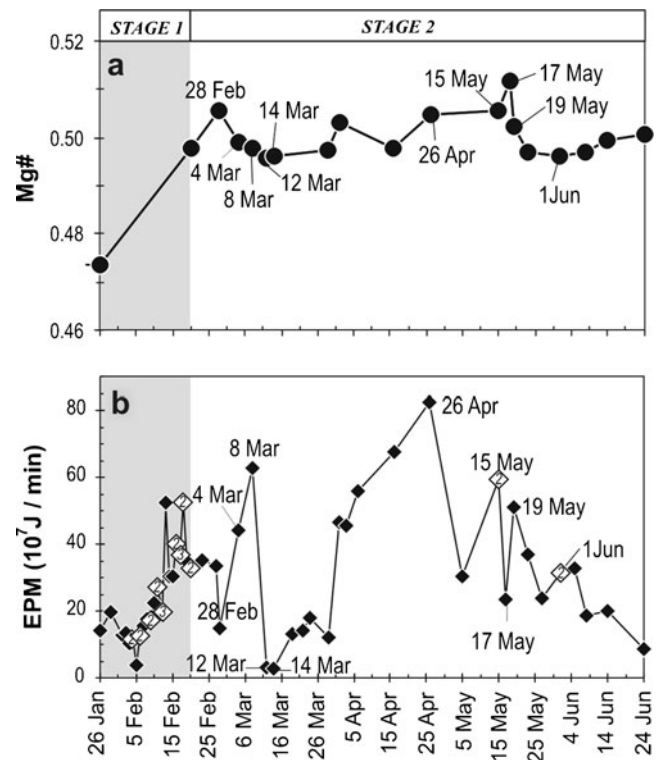


Fig. 7 Temporal variation during the 2000 SE Crater eruption of: **a** $Mg\# = Mg/(Mg + Fe^{2+})$ moles, assuming $Fe^{3+}/Fe^{2+} = 0.2$ and **b** EPM (Energy radiated as tremor Per Minutes, 10^7 J/min, data from Alparone et al. 2003). The dates of the lava fountains discussed in the text are indicated. If more than one fountain a day occurred, the average EPM value is plotted with an open diamond containing the number of lava fountains for that day

et al. 2003). To better highlight possible relationships among volcanological features, seismic energy and compositional data throughout the whole eruptive period, we introduce the parameter EPM (Energy Per Minute), calculated as the ratio between seismic energy radiated as tremor during a lava fountain episode (10^7 Joule; Alparone et al. 2003) and its duration (in minutes) (Fig. 7b). This parameter allows comparison of intensity among episodes having different durations.

During stage 1 the 2000 eruption was characterized by very frequent fountains (up to 3 events/day) associated with initially low values of EPM ($<20 \cdot 10^7$ J/min) which gradually increased from 5 February up to 18 February (Fig. 7b). The rising EPM value is due to the fairly constant seismic energy release (see Fig. 4b of Alparone et al. 2003) coupled with a decline in fountain durations (see Table 1 of Alparone et al. 2003). In the same period also the tremor amplitude (RD) increased with time (see Fig. 3 of Alparone et al. 2003). Stage 1 then, was characterized by the occurrence of very frequent, short-lived lava fountains, with tremor amplitude increasing over time, and whose products show the strongest and most rapid compositional variation of the entire eruption, becoming significantly

more mafic (Figs. 6 and 7a). In our opinion, all these observations concur to infer that during the first stage of the 2000 activity, the steady state condition existing in the SE Crater's reservoir after the end of the 1999 sub-terminal eruption rapidly changed due to the supply of a deeper, more primitive and volatile-rich magma. This magma progressively exsolved gases which concentrated in the uppermost zone of the reservoir, triggering the lava fountaining (see next sections). Furthermore the new magma started to mix with an already stored and more evolved one (see next section), causing the shift towards more mafic compositions of the erupted products. The rapid variation of volcanological and seismic activity during stage 1, leads us to conclude that magma ascent reached its climax on 20 February.

During stage 2 (Fig. 7b), the Energy per minute (EPM) pattern was very variable and on the whole higher than the average value ($EPM=24 \cdot 10^7$ J/min) measured in the previous stage. The EPM mostly correlated with volcanological parameters: it significantly increased during the 4 and 8 March, 26 April and 15 May lava fountains which, according to camera and field observations (Alparone et al. 2003), were very powerful, while the EPM abruptly dropped during the scarcely explosive 12 and 14 March episodes (Fig. 7b). During stage 2, there is no point-to-point temporal correlation between the composition of the emitted products (Fig. 7) and the EPM of a lava fountain. In other words, lava fountains with high energy rate (EPM) generally did not emit a more volatile-rich and mafic magma. For example, the 26 April lava fountain with the highest EPM of the 2000 eruption, produced magma not significantly more primitive than previously erupted ones (Fig. 7a and b). Conversely, the most primitive products of the 2000 eruption were erupted on 17 May during a lava fountain which was significantly less forceful than the other ones occurring in May; finally, also the relatively highly mafic compositions of products erupted on 28 February were associated with a significant negative trough in EPM.

Magmatic processes in the SE Crater's plumbing system and inferences regarding its geometry

Crystal-liquid fractionation does not greatly affect incompatible trace element ratios, therefore the significant differences between Rb/Nb and $K/Th \cdot 10^3$ values of the most evolved trachybasalts erupted on 26 January and of the most primitive products emitted on 15–17 May (Fig. 6d and e) suggest the involvement of other petrogenetic processes. This conclusion is also qualitatively supported by the distribution of 2000 FF products, which do not follow the horizontal trend (see arrow in Fig. 8) modelled for fractional crystallization starting from

the most primitive magma of the 2000 SE Crater eruption (point 1 in Fig. 8, i.e. the average composition of samples 150500A and 180500A).

Alternatively, the compositional variability of 2000 FF products has been modelled assuming a mixing process (Langmuir et al. 1978) between an evolved magma stored in the SE Crater's reservoir (represented by point 2 in Fig. 8, i.e. the average composition of samples 260100A and 260100B) and a new, more primitive and volatile-rich magma entering the reservoir (represented by the above described point 1 in Fig. 8). Most of the 2000 FF products are the result of a mixing process (Fig. 8) which involves up to about 60% of the 15–17 May component (point 1) and 40% of the 26 January one (point 2). In detail, the products emitted up to 15–17 May cluster close to the most primitive end member (point 1), whilst lavas emitted after 15–17 May and until the end of the eruption (see samples in the box of Fig. 8) lie along a portion of the mixing line closer to the more evolved end member (point 2). Once the 2000 SE Crater eruption had finished, the composition of the products progressively shifted (see sample 28 Aug in Fig. 8) towards point 2 and finally, on 30 November 2000, erupted pyroclasts were compositionally very close to the volcanics emitted on 26 January (see sample 30 Nov in Fig. 8) and also in 1997–98 from the SE Crater. This circumstance suggests that, by the end of November, the contribution of the deep magma intruding the SE Crater's reservoir had ended and the resident magma was able to re-establish the composition it had before (1997–98) and at the eruption onset (26 January).

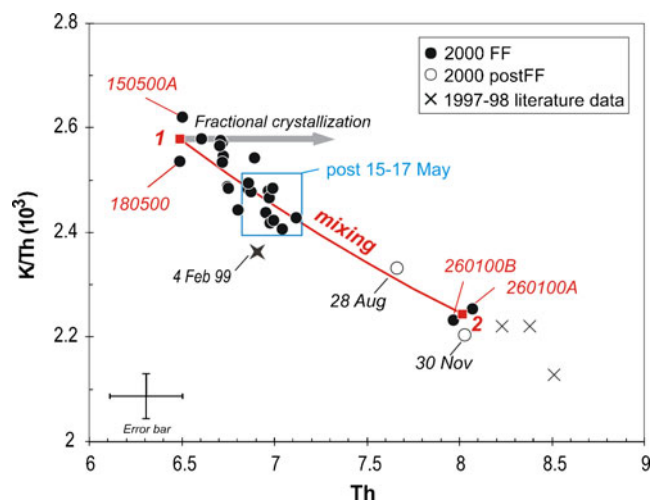


Fig. 8 $K/Th \cdot 10^3$ vs. Th for the products of the 2000 SE Crater eruption compared with 1997–98 literature data (La Delfa et al. 2001; Corsaro and Pompilio 2004; Corsaro, 2010 unpublished work). The end members of the mixing curve are indicated as 1: the average composition of samples 150500A and 180500A, and 2: the average composition of samples 260100A and 260100B. For details see the text

The occurrence of a progressive mixing process between magmas as described above is also supported by petrographic lines of evidences (see section [Petrography and Mineral chemistry](#)). The magma erupted on 26 January is highly porphyritic, plagioclase-rich and contains minerals with fairly evolved and almost homogeneous compositions. The effects of its mixing with a more primitive magma become increasingly more evident in the products erupted from March–April and finally on 15 May. In fact, with respect to 26 January, later lavas/pyroclasts are less porphyritic and richer in mafic minerals. Furthermore, their plagioclase and olivine compositional ranges are wider and more primitive and also oscillatory and reverse zoning in frequently anhedral crystals, are common.

Others events of magma recharge also occurred in the years preceding the 2000 eruption, as is highlighted by the petrography and composition of the products erupted at the onset (on 4 February) of the 1999 sub-terminal eruption. They, in fact, are less porphyritic, richer in mafic minerals (see [Petrography and mineral chemistry section](#)) and more primitive (see 4 Feb 99 sample in Figs. 5 and 8) than products emitted from the SE Crater in the period 1997–98. It is noteworthy that the magma erupted on 4 February 1999 was more evolved than the 15–17 May 2000 one, which therefore represents the most primitive magma erupted by SE Crater since 1996, when the crater resumed its Strombolian activity after the conclusion of the long-lasting 1991–93 flank effusive eruption.

The geometry (shape and size) of the reservoir involved in the 2000 activity of SE Crater may be qualitatively inferred by analyzing the patterns of geochemical parameters with time (Pietruszka and Garcia 1999). On this basis, the composition of our samples indicates fairly regular time-related trends with restricted variability, except for the products erupted on 26 January. This circumstance implies the existence of a magma reservoir with a simple geometry and a small volume. Here the mixing process invoked to explain the compositional variability throughout the eruption might occur and both the stored and new uprising magma might efficiently mix and homogenize. Alternatively, the hypothesis of a more complex reservoir (i.e. a plexus of dikes) is difficult to fit with our compositional data. This geometry enhances the development of magma compositional heterogeneity and each lava fountain, tapping such a reservoir, would maintain compositional differences, preventing the geochemical temporal pattern that characterizes our samples.

In order to estimate the volume of the magma reservoir involved in this eruption, we assume that its size, at least for the liquid part, corresponds to the total volume of magma erupted during the 2000 eruption ($15\text{--}20 \times 10^6 \text{ m}^3$ lava and $2\text{--}3 \times 10^6 \text{ m}^3$ of tephra; Alparone et al. 2003). By correcting the magma volume for its bulk vesicularity

(respectively 20% for lava and 50% for tephra), the volume of magma as dense rock equivalent (DRE) stored in the SE Crater shallow plumbing system was between 13 and $17.5 \times 10^6 \text{ m}^3$. Only a small part of this magma resided in the conduit and its volume should have ranged between 1.4 and $3.6 \times 10^4 \text{ m}^3$ if it had a radius of 5–8 m (Bonaccorso 2006) and a length of about 1800 m, which is the depth where the roof of the SE Crater's reservoir has been located by Spilliaert et al. (2006).

Dynamic model of the 2000 South–East Crater eruption

Previous authors (La Delfa et al. 2001) explained the 'periodic eruptions' occurring at the SE Crater in 1998 in terms of cyclic replenishments and partial emptying of a shallow magma chamber below this summit crater. In our opinion, this model implies that regular compositional patterns would be difficult to preserve in the products of different lava fountains. The recurrent magma input/output during each episode, in fact, reasonably modifies the chemical-physical characteristics of the stored magma and consequently the composition of the erupted products becomes variable and irregular with time. Starting from this consideration, we therefore argue that the model of La Delfa et al. (2001) does not fit our geochemical data which, on the contrary, show fairly regular distributions (Figs. 6 and 7a). Instead, and with the support of petrography, mineral chemistry and major/trace elements of bulk rocks, integrated with volcanological/seismic observations, we propose a different dynamic model for the 2000 SE Crater lava fountains eruption. It points to one significant event of magma recharge within the reservoir, which was followed by mixing of the new intruding magma with the one already stored inside.

Hence, we argue that before the onset of the 2000 lava fountaining, an evolved trachybasalt (represented by the samples erupted on 26 January), probably inherited from the sub-terminal SE Crater eruption started on 4 February 1999, was stored in the SE Crater reservoir. There it cooled and degassed, crystallizing abundant minerals, mainly plagioclase. Then, a more primitive and volatile-rich magma ascended from depth and intruded the reservoir. Possibly its efficient degassing caused the formation of a foam layer, whose collapse forced the expulsion of the resident magma, driving the first lava fountain, on 26 January. During stage 1, the magma supply in the SE Crater's reservoir not only influenced the eruptive style, enhancing the frequency and energy rate release of lava fountains, but also modified the composition of the already stored magma which efficiently mixed with the new one and, in less than one month, became significantly more primitive. During stage 2, the new magma entered the SE Crater's reservoir

and continued to mix with the stored one. Consequently the ‘imprint’ of the recharging magma is increasingly evident in the products erupted up to 15–17 May, when the most mafic magma of the entire eruption was erupted. Afterward and up to 24 June, slightly more evolved lavas were emitted (Figs. 6 and 8), suggesting that the contribution of the new magma gradually diminished, probably due to the lack of further supply from depth, and/or to a different efficiency of the mixing process.

In the proposed model, the mixing process between different magmas within the reservoir proceeded undisturbed by the occurrence of lava fountaining, causing regular compositional variations of the erupted products with time. It follows that episodic lava fountains during the 2000 SE Crater eruption were not driven by the recurrent refilling of the reservoir (La Delfa et al. 2001) but rather, as suggested in the next section, by the dynamics of the bubbles inside the reservoir itself.

To investigate the behaviour of the SE Crater’s reservoir on a wider temporal scale, including the months subsequent to the 2000 eruption, we stress (Fig. 8) that the products erupted after the end of the 2000 lava fountains, became progressively more evolved and in November resembled the 26 January ones (Fig. 8). This circumstance suggests that the magma residing in the reservoir takes about 10 months to restore the composition it had before new magma was supplied. Such a relatively short time for re-establishing a former composition is probably due to the simple geometry and small size of the reservoir, as already discussed in the previous section, and to the efficiency of the mixing process. Significantly, the restored magma composition is very similar to the 1997–98 SE Crater one (Fig. 8) suggesting that, at least from 1997 to 2000, the balance between magma input/output inside the SE Crater’s plumbing system and magmatic processes has been able to preserve a magma with a buffered composition.

Gas-magma dynamics driving the lava fountains

In the literature, there are two physical models describing basaltic lava fountaining. The Collapsing Foam (CF) model (Jaupart and Vergnolle 1988, 1989; Vergnolle and Jaupart 1990) implies the existence of a reservoir where magma exolves volatiles. They accumulate at the top of the storage zone and form a foam layer whose instantaneous and massive collapse causes the bubble coalescence and triggers an annular flow feeding a lava fountain. Alternatively, the Rise Speed Dependent (RSD) model (Parfitt 2004 and references therein) does not require a reservoir where magma degasses; a lava fountain is triggered by an increase in the magma rate and volatile flux, associated with rapid

volatile exsolution and bubble coalescence during magma ascent (syneruptive degassing).

Following the latter model, if an increase of magma rate (and volatile flux) drove each lava fountain during the 2000 SE Crater eruption, at least the most powerful episodes should be associated with the fast ascent of new, volatile-rich and relatively more primitive magma from depth. This circumstance should imply a point-to-point direct correlation between Energy per minute (EPM) and a compositional parameter indicative of magma ‘primitiveness’. Our data (Fig. 7) however, show that this correspondence does not exist and, as already discussed, temporal patterns of geochemical parameters are regular (Figs. 6 and 7a).

We thus conclude that the RSD model, at least qualitatively, does not allow matching the seismic/volcanological information with the compositional trends of the 2000 eruption of SE Crater. As an alternative to this hypothesis, we contend that the CF model provides a better framework to explain our data. It implies the existence of a magmatic reservoir where the discussed mixing process between magmas may occur. Furthermore, since the explosive activity is essentially driven by the dynamics of bubbly melt at the top of the reservoir, the mixing process may advance independently from lava fountaining and produce the regular geochemical trends observed in the erupted products. Finally, according to the CF model (Jaupart and Vergnolle 1988, 1989; Vergnolle and Jaupart 1990), we may explain the episodic nature of the eruption by the behaviour of the foam layer trapped at the top of the reservoir. When the foam becomes unstable, a large gas volume is released into the volcanic conduit, leading to lava fountaining. Afterward, the process of bubble accumulation resumes, causing formation of a new foam in the upper reservoir which ultimately produces a new lava fountain episode.

Our results, reinforcing the CF model as the driving mechanism of episodic lava fountaining eruptions at Mt. Etna, are consistent with the scenarios proposed for the 2000 SE Crater eruption by i) Alparone et al. (2003), who suggested that during each lava fountain episode, initial gas exsolution and bubble migration led to the formation of a foam layer in the upper portion of a small magma chamber, ii) Allard et al. (2005) and Spilliaert et al. (2006), who invoked the growth and collapse of a foam located at 1.5–1.8 km depth to explain the formation of a lava fountain, and finally iii) Polacci et al. (2006), who inferred a foam collapse associated with a minor syneruptive degassing to explain the dynamics of the lava fountains. The collapsing foam model has also been proposed as the main process controlling the formation of lava fountains at SE Crater in 2001 during the months preceding the flank eruption (Vergnolle 2008; Vergnolle and Ripepe 2008).

Conclusions

The integration of a large set of volcanological, seismic and petrochemical data has provided an opportunity to investigate the magmatic processes governing the 2000 eruption at Mt. Etna, and to propose a model consistent with the episodic lava fountaining

In particular, we demonstrated how the entry of a new, more primitive and volatile-rich magma to the SE Crater's reservoir, modified its steady state conditions, enhancing an efficient mixing with an evolved magma already stored inside it, thereby triggering and sustaining the episodic lava fountaining eruption for about 5 months.

We also suggest that the periodic lava fountains were essentially controlled by the collapse of a foam layer accumulated at the top of the SE Crater's reservoir which was rebuilt prior to each episode. Indeed, such a model better fits the dynamics of magma during its fast ascent on the basis of our compositional data, supporting the episodic nature of the lava fountains.

Finally, we think that the study and interpretation of lava fountaining from the summit craters of Mt. Etna should be completed by better investigating occasional lava fountains as well, whose triggering mechanism and eruptive dynamics are not necessarily the same as those discussed in this paper for the episodic lava fountaining of the 2000 eruption.

Acknowledgments We are deeply grateful to L. Lodato for having shared field surveys and collecting most of the samples with D. Andronico. The paper has greatly benefited from the suggestions of S. Alparone, R. Cioni and J.D.L. White. We greatly appreciated the constructive comments made by N. Métrich and an anonymous reviewer. Our thanks to L. Messina for preparing powder for rock analyses. Geochemical analyses were funded by Istituto Nazionale di Geofisica e Vulcanologia, sezione di Catania for the monitoring activity of Sicilian active volcanoes.

References

- Allard P, Burton M, Murè F (2005) Spectroscopic evidence for a lava fountain driven by previously accumulated magmatic gas. *Nature* 433:407–410
- Alparone S, Andronico D, Lodato L, Sgroi T (2003) Relationship between tremor and volcanic activity during the Southeast Crater eruption on Mount Etna in early 2000. *J Geophys Res* 108: B52241. doi:10.1029/2002JB001866
- Alparone S, Andronico D, Giammanco S, Lodato L (2004a) A multidisciplinary approach to detect active pathways for magma migration and eruption in a basaltic volcano: the upper southern flank of Mt. Etna (Sicily, Italy) before the 2001 eruption. *J Volcanol Geotherm Res* 136:121–140
- Alparone S, Andronico D, Sgroi T (2004b) Characteristics of the volcanic tremor at Southeast Crater, Etna (Italy), during a long series of explosive paroxysms. IAVCEI General Assembly 2004, Pucón – Chile, November 14–19
- Alparone S, Andronico D, Sgroi T, Ferrari F, Lodato L, Reitano D (2007) Alert system to mitigate tephra fallout hazards at Mt. Etna Volcano, Italy. *Nat Hazards*. doi:10.1007/s11069-007-9120-7
- Andronico D, Cristaldi A, Scollo S (2008) The 4–5 September 2007 lava fountain at South–East Crater of Mt Etna, Italy. *J Volcanol Geotherm Res* 173:325–328
- Andronico D, Spinetti C, Cristaldi A, Buongiorno MF (2009a) Observations of Mt. Etna volcanic ash plumes in 2006: an integrated approach from ground-based and polar satellite NOAA-AVHRR monitoring system. *J Volcanol Geotherm Res*. doi:10.1016/j.jvolgeores.2008.11.013
- Andronico D, Scollo S, Cristaldi A, Ferrari F (2009b) Monitoring ash emission episodes at Mt. Etna: the 16 November 2006 case study. *J Volcanol Geotherm Res* 180(2–4):123–134. doi:10.1016/j.jvolgeores.2008.10.019
- Behncke B, Neri M, Pecora E, Zanon V (2006) The exceptional activity and growth of the Southeast Crater, Mount Etna (Italy), between 1996 and 2001. *Bull Volcanol* 69(2):149–173. doi:10.1007/s00445-006-0061-x
- Bonaccorso A (2006) Explosive activity at Mt. Etna summit craters and source modelling by using high-precision continuous tilt. *J Volcanol Geotherm Res* 158:221–234
- Corsaro RA, Pompilio M (2004) Magmatic processes in the shallow plumbing system of Mt. Etna as recorded by compositional variations in volcanics of recent summit activity (1995–1999). *J Volcanol Geotherm Res* 137(1–3):55–71
- Giordano D, Polacci M, Papale P, Caricchi L (2010) Rheological control on the dynamics of explosive activity in the 2000 summit eruption of Mt. Etna. *Solid Earth* 1:61–69
- Jarosewich E, Nelen JA, Norberg JA (1980) Reference samples for electron microprobe analysis. *Geostand Newsl* 4(1):43–47
- Jaupart C, Vergnolle S (1988) Laboratory models of Hawaiian and Strombolian eruptions. *Nature* 331:58–60
- Jaupart C, Vergnolle S (1989) The generation and collapse of foam layer at the roof of a basaltic magma chamber. *J Fluid Mech* 203:347–380
- La Delfa S, Patané G, Clocchiatti R, Joron JL, Tanguy JC (2001) Activity of Mount Etna preceding the February 1999 fissure eruption: inferred mechanism from seismological and geochemical data. *J Volcanol Geotherm Res* 105:121–139
- Langmuir CH, Vocke RD Jr, Hanson GN, Hart SR (1978) A general mixing equation with applications to Icelandic basalts. *Earth Planet Sci Lett* 37(3):380–392. doi:10.1016/0012-21X(78)90053-5
- Le Maitre RW (Ed.) (2002) *Igneous rocks. A classification and glossary of terms*, 2nd edn. Recommendations of the IUGS Subcommission on the Systematics of Igneous Rocks, pp. 236, Cambridge University Press
- Miraglia L (2006) Valutazione dell'accuratezza e della precisione delle analisi eseguite con il sistema analitico SEM-EDS su standard internazionali di minerali e vetri, Report UFGV2006/115, pp. 5, Istituto Nazionale Geofisica e Vulcanologia, Catania, Italy
- Parfitt EA (2004) A discussion of the mechanisms of explosive basaltic eruptions. *J Volcanol Geotherm Res* 134(1–2):77–107
- Parfitt EA, Wilson L (1994) The 1983–86 Pu'u'Ō'o eruption at Kilauea Volcano, Hawaii: a study of dike geometry and eruption mechanisms for a long-lived eruption. *J Volcanol Geotherm Res* 59:179–205
- Pietruszka AJ, Garcia MO (1999) The size and shape of Kilauea Volcano's summit magma storage reservoir; a geochemical probe. *Earth Planet Sci Lett* 167(3–4):311–320
- Polacci M, Corsaro R, Andronico D (2006) Coupled textural and compositional characterization of basaltic scoria: Insights into the transition from Strombolian to fire fountain activity at Mount Etna, Italy. *Geology* 34(3):201–204. doi:10.1130/G223181.1
- Privitera E, Sgroi T, Gresta S (2003) Statistical analysis of intermittent volcanic tremor associated with the September 1989 summit

- explosive eruptions at Mount Etna, Sicily. *J Volcanol Geotherm Res* 120:235–247
- Richter DH, Eaton JP, Murata KJ, Ault WU, Kivoy HL (1970) Chronological narrative of the 1959–60 eruption of Kilauea volcano, Hawaii. *US Geological Survey Professional Papers* 537:1–70
- Spilliaert N, Metrich N, Allard P (2006) S-Cl-F degassing pattern of water-rich alkali basalt: modelling and relationship with eruption styles on Mount Etna volcano. *Earth Planet Sci Lett* 248:772–786
- Swanson DA, Duffield WA, Jackson DB, Peterson DW (1979) Chronological narrative of the 1969–71 Mauna Ulu eruption of Kilauea volcano, Hawai'i. *U.S. Geol Surv Prof Pap* 1056
- Vergnolle S (2008) From sound waves to bubbling within a magma reservoir: comparison between eruptions at Etna (2001, Italy) and Kilauea (Hawaii). In: Lane SJ & Gilbert JS (eds) *Fluid motions in volcanic conduits: a source of seismic and acoustic signals*. Geological Society, London, Special Publications, 307:125–146
- Vergnolle S, Jaupart C (1990) The dynamics of degassing at Kilauea volcano, Hawaii. *J Geophys Res* 95(B3):2793–2809
- Vergnolle S, Ripepe M (2008) From Strombolian explosions to fire fountains at Etna Volcano (Italy): what do we learn from acoustic measurements? In: Lane SJ & Gilbert JS (eds) *Fluid Motions in Volcanic Conduits: A Source of Seismic and Acoustic Signals*. Geological Society, London, Special Publications, 307:103–124
- Wolfe EW, Garcia MO, Jackson DB, Koyanagi RY, Neal CA, Okamura AT (1987) The Pu' u ' O' o eruption of Kilauea volcano, episodes 1–20, January 3, 1983, to June 8, 1984. Chapter 17, *US Geol Surv Prof Pap* 1350
- Wolfe EW, Neal CA, Banks NG, Duggan TJ (1988) Geological observations and chronology of eruptive events. Chapter 1, *US Geol Surv Prof Pap* 1463